

Generation of clinical 177Lu SPECT/CT images based on Monte Carlo simulation with GATE

Gunjan Kayal, Maxime Chauvin, Alex Vergara Gil, Naomi Clayton, Ludovic Ferrer, Tumelo Moalosi, Peter Knoll, Lara Struelens, Manuel Bardiès

▶ **To cite this version:**

Gunjan Kayal, Maxime Chauvin, Alex Vergara Gil, Naomi Clayton, Ludovic Ferrer, et al.. Generation of clinical 177Lu SPECT/CT images based on Monte Carlo simulation with GATE. Physica Medica, 2021, 85 (4), pp.24-31. 10.1016/j.ejmp.2021.04.002 . hal-03304053

HAL Id: hal-03304053
https://hal.science/hal-03304053

Submitted on 25 Jan 2022

HAL is a multi-disciplinary open access archive for the deposit and dissemination of scientific research documents, whether they are published or not. The documents may come from teaching and research institutions in France or abroad, or from public or private research centers.

L'archive ouverte pluridisciplinaire **HAL**, est destinée au dépôt et à la diffusion de documents scientifiques de niveau recherche, publiés ou non, émanant des établissements d'enseignement et de recherche français ou étrangers, des laboratoires publics ou privés.

Physica Medica 85 (2021) 24–31

Contents lists available at ScienceDirect

Physica Medica

journal homepage: www.elsevier.com/locate/ejmp

Original paper

Generation of clinical ^{177}Lu SPECT/CT images based on Monte Carlo simulation with GATE

Gunjan Kayal [a,b,*], Maxime Chauvin [a], Alex Vergara-Gil [a], Naomi Clayton [a], Ludovic Ferrer [c,d], Tumelo Moalosi [e], Peter Knoll [f], Lara Struelens [b], Manuel Bardiès [g,h]

[a] CRCT, UMR 1037, INSERM, Université Toulouse III Paul Sabatier, France
[b] SCK CEN, Belgian Nuclear Research Centre, Mol, Belgium
[c] ICO René Gauducheau, Medical Physics Department, Saint Herblain, France
[d] CRCINA, UMR 1232, INSERM, Nantes, France
[e] Stellenbosch University, Tygerberg Hospital, South Africa
[f] Dosimetry and Medical Radiation Physics, International Atomic Energy Agency, Austria
[g] Département de Médecine Nucléaire, Institut Régional du Cancer de Montpellier (ICM), Montpellier F-34298, France
[h] IRCM, UMR 1194 INSERM, Université de Montpellier and Institut Régional du Cancer de Montpellier (ICM), Montpellier F-34298, France

ARTICLE INFO

Keywords:
Clinical dosimetry
DosiTest
SPECT/CT
GATE Monte Carlo modelling

ABSTRACT

Purpose: Patient-specific dosimetry in MRT relies on quantitative imaging, pharmacokinetic assessment and absorbed dose calculation. The DosiTest project was initiated to evaluate the uncertainties associated with each step of the clinical dosimetry workflow through a virtual multicentric clinical trial. This work presents the generation of simulated clinical SPECT datasets based on GATE Monte Carlo modelling with its corresponding experimental CT image, which can subsequently be processed by commercial image workstations.
Methods: This study considers a therapy cycle of 6.85 GBq ^{177}Lu-labelled DOTATATE derived from an IAEA-Coordinated Research Project (E23005) on "Dosimetry in Radiopharmaceutical therapy for personalised patient treatment". Patient images were acquired on a GE Infinia-Hawkeye 4 gamma camera using a medium energy (ME) collimator. Simulated SPECT projections were generated based on experimental time points and validated against experimental SPECT projections using flattened profiles and gamma index. The simulated projections were then incorporated into the patient SPECT/CT DICOM envelopes for processing and their reconstruction within a commercial image workstation.
Results: Gamma index passing rate (2% – 1 pixel criteria) between 95 and 98% and average gamma between 0.28 and 0.35 among different time points revealed high similarity between simulated and experimental images. Image reconstruction of the simulated projections was successful on HERMES and Xeleris workstations, a major step forward for the initiation of a multicentric virtual clinical dosimetry trial based on simulated SPECT/CT images.
Conclusions: Realistic ^{177}Lu patient SPECT projections were generated in GATE. These modelled datasets will be circulated to different clinical departments to perform dosimetry in order to assess the uncertainties in the entire dosimetric chain.

1. Introduction

Molecular radiotherapy (MRT) is a systemic cancer radiotherapy, where a radiopharmaceutical binds specifically to cancer targets to selectively irradiate the tumour cells while sparing healthy tissues. Dosimetry permits the optimisation of the treatment by calculating the absorbed dose from the irradiation delivered to the tumour targets as well as the healthy tissues. Clinical dosimetry in molecular radiotherapy relies on determining the spatial distribution of the radiopharmaceutical in different organs by imaging at different times (*quantitative imaging*); determining the total number of radioactive decays by integrating activity over time post injection (*pharmacokinetic assessment*) and calculating the *absorbed dose* based on radioactive decay distribution, energy emitted per decay for the radioisotope, and radiation interactions within

* Corresponding author.
E-mail addresses: gunjan.kayal@inserm.fr, gunjan.kayal@sckcen.be (G. Kayal).

https://doi.org/10.1016/j.ejmp.2021.04.002
Received 3 December 2020; Received in revised form 4 March 2021; Accepted 6 April 2021
Available online 3 May 2021
1120-1797/© 2021 Associazione Italiana di Fisica Medica. Published by Elsevier Ltd. This is an open access article under the CC BY-NC-ND license (http://creativecommons.org/licenses/by-nc-nd/4.0/).

propagating media. The global accuracy of clinical dosimetry relies on the accuracy of each of these steps [2]. This is challenging, as some steps cannot be validated experimentally.

Significant heterogeneities can be observed in current clinical dosimetry practice, at least in part related to the implementation of widely differing dosimetry protocols.

The DosiTest project [3,4] was initiated to evaluate the uncertainties associated with each step of the clinical dosimetry workflow and to propose standardised approaches to clinical dosimetry in MRT. The aim is to create a 'virtual' multicentric clinical dosimetry trial by circulating virtual patient datasets to the different participating centres and allowing them to process these datasets according to their dosimetric approach *as if they were patients locally enrolled in their own nuclear medicine department*. Then, by obtaining the absorbed dose results along with a range of intermediate results from each centre, the heterogeneity in the clinical procedures implemented in different centres can be assessed and the uncertainties associated to each step of the dosimetric workflow evaluated.

To take account of this heterogeneity and to allow each centre to perform dosimetry according to their local protocol, it is important to generate image data according to their own requirements in terms of acquisition settings, image format, time sampling, etc. Furthermore, the resulting datasets (planar, or SPECT/CT projections) should be processed in the clinical workstations installed in each nuclear medicine facility.

An essential asset for the development of such an approach is the implementation of Monte Carlo modelling to generate clinical images based on a virtual, fully characterised patient. As nuclear interactions are stochastic in nature, Monte Carlo simulations have become ubiquitous for modelling radiation transport along with medical imaging systems and techniques [5–7]. It is used both in the context of scintigraphic image generation as well as absorbed dose calculations. Various Monte Carlo codes are available today for modelling planar and SPECT imaging [8]. GATE [9] is one of the most popular simulation toolkits for modelling emission tomography. Along with the ability to model complex geometries and imaging configurations, GATE incorporates the modelling of time-dependent processes such as geometry movements, decay kinetics and dead time modelling. GATE can also be used to compute the absorbed doses delivered by radiopharmaceuticals [10] and was selected for the development of the DosiTest project.

The first phase of the project is the generation of simulated clinical images (planar and/or SPECT) at different time points post injection, based on a patient geometry and pharmacokinetics for which dosimetry can be fully characterised.

The clinical situation of Peptide Receptor Radionuclide Therapy (PRRT) using FDA and EMA approved radiopharmaceutical Lutathera® was considered.

As part of DosiTest feasibility studies, 2D planar scintigraphic imaging after Lutathera® administration has been already addressed by Costa *et al.* [11]. Whole-body acquisitions based on the *XCAT model* and a hypothetical ^{177}Lu-DOTATATE pharmacokinetics were modelled on a Siemens Symbia T2 gamma camera model. More recently, the International Atomic Energy Agency (IAEA) initiated a Coordinated Research Project (CRP) to support the standardisation and dissemination of dosimetric methods in nuclear medicine therapy [1]. This project (IAEA CRP project E23005 on "Dosimetry in Radiopharmaceutical therapy for personalised patient treatment") involves the circulation, within several medical physics departments, of SPECT/CT images obtained from a *clinical* situation of ^{177}Lu-labelled DOTATATE (Lutathera®) therapy. This experimental dataset was used as the base for generating simulated SPECT/CT.

This work focuses on the generation of SPECT/CT images of a *patient* undergoing Lutathera® treatment. Tomographic projections with a GE Infinia Hawkeye SPECT/CT gamma camera were generated using GATE Monte Carlo simulation. These simulated projections were integrated in a SPECT/CT DICOM header file to enable commercial image workstations to access the simulated dataset as if they were real patient datasets. These images will then be circulated to different clinical centres to perform dosimetry thus allowing to determine the heterogeneity of the applied clinical procedures.

2. Methods

Experimental images were obtained from Tygerberg Hospital, South Africa. A dual-headed Infinia Hawkeye 4 SPECT/CT (GEHC, Milwaukee, USA) with a medium energy collimator was used. Patient CT and SPECT projections were obtained from the same centre with the same gamma camera and acquisition parameters at 1 h, 4 h, 24 h, 48 h and 96 h post injection along with calibration phantom images.

CT system containing 4-slice detector arrays rotates at 2.6 revolutions per minute. Other CT scan parameters include; 10 mm slice thickness, tube voltage of 140 kVp, tube current of 2.5 mA and helical scan with a fixed pitch of 1.9 mm per revolution. CT slices were acquired in a 256 × 256 matrix with pixel size of 2.209 × 2.209 mm^2.

SPECT projections were acquired in *auto-contour mode* with matrix size of 128 × 128 (pixel size 4.418 × 4.418 mm^2), 15 s per projection and one energy window of 208 keV ± 20%.

To enable clinical quantitative imaging, SPECT images of a water-filled IEC NEMA body phantom were acquired. A uniform ^{177}Lu activity concentration of 250 kBq/ml in 3 spheres of diameter 22 mm, 28 mm and 37 mm respectively and 32.26 kBq/ml in the phantom (total volume of 10200 ml) was used.

Further, reconstruction was also performed by the centre on a HERMES workstation using the OSEM algorithm (3 iterations, 15 subsets) and 0.8 cm Gaussian post-filter corrected for attenuation (using low dose CT) and in-built Monte Carlo scatter correction. A calibration factor of 4.53 ± 0.22 cps/MBq derived from experiments was used for activity quantification in experimental patient images.

2.1. Gamma camera model

Modelling or simulation of SPECT imaging in GATE requires the development of a gamma camera model along with the modelling of the patient (or phantom).

Gamma camera modelling in GATE involves the modelling of the individual components of the gamma camera i.e. the collimator (holes, septa and collimator cover), crystal and the back-compartment (light guide, photomultiplier tubes (PMTs) and associated electronics). The GE Infinia Hawkeye SPECT/CT gamma camera model was derived from the previous work of Garcia *et al.* [4]. This dual headed gamma camera model was designed according to the manufacturer's specifications and consists of 9.5 mm NaI crystal with an aluminium cover, a medium energy lead collimator, glass back-compartment and lead shield [12].

The auto-contouring motion of the gamma camera was modelled by extracting information such as radial position, acquisition starting angle and the angular step from the experimental acquisitions. These parameters were then converted in a series of translations and rotations and transformed into an ascii file compatible with GATE in order to depict the independent movement of each gamma camera head around the patient.

Simulated SPECT projections were generated based on the experimental image characteristics (same matrix and pixel size).

2.2. Calibration: the phantom model

The calibration factor obtained experimentally cannot be directly used for simulated images, as the gamma camera model sensitivity is not always equivalent to that of the real gamma camera. A virtual calibration experiment was designed to generate a camera model calibration factor.

Therefore, calibration SPECT images for the NEMA IEC phantom and same acquisition parameters were modelled using GATE to derive a

Table 1
Densities of different VOIs derived from the average density in the patient.

Volume of interest (VOIs)	Densities (g/cm^3)
Lungs	0.362
Liver	1.019
Bones	1.093
Left Kidney	0.999
Right Kidney	1.003
Spleen	0.991
Tumour	1.020
Remainder of the body	0.941

Table 2
Mean volumes for each VOI along with its maximum deviation from mean among different time points.

Volume of interest (VOIs)	Mean volumes (cm^3)	Standard deviation (cm^3)
Lungs	1524.2	67.2
Liver	1326.6	32.3
Bones	1301.7	69.1
Left Kidney	183	9.7
Right Kidney	194	12.7
Spleen	121	4.1
Tumour	239	23.78
Remainder of the body	19077	395.8

simulated calibration factor.

We used a uniform activity concentration of 11.12 kBq/ml in the whole phantom as was done by Zhao *et al.* [13]. This corresponds to a total activity of 107.83 MBq in the phantom, i.e. an activity in the range of that used experimentally.

2.3. Patient model

2.3.1. CRP patient

The third therapy cycle for a patient in Tygerberg Hospital, South Africa was considered with an injected activity of 6.85 ± 0.34 GBq Lutathera®. Acquisition setup and parameters were presented earlier.

The reconstructed SPECT along with corresponding CT were imported into OpenDose3D [14], a specific clinical dosimetry module based on 3D Slicer [15,16] to assess activity in various volumes of interest. Experimental calibration factor (4.53 ± 0.22 cps/MBq) were entered in the software. The segmentation of different volumes of interest (VOIs) was performed in OpenDose3D using the 3DSlicer Segment Editor tool. VOIs including the lungs, bones, left and right kidneys, spleen, liver and the remainder of the body were defined and segmented on the CT while a tumour present in the liver was segmented on the SPECT image. This process was performed for every time point.

The CT was resampled to the SPECT resolution using Lanczos interpolation [17] and further rescaled to generate density matrices. Each VOI was further labelled and a labelled map was exported from Slicer3D toolkit to be used for modelling patient geometry. The patient volume was masked and zero activity assigned to the regions outside the patient boundary.

2.3.2. From CRP patient to digital patient model

The segmented and labelled patient CT maps were used to define the geometry of each volume of interest along with its composition. Each VOI composition was set according to the NIST material database (available as Supplementary material) and average densities was derived from the patient CT (Table 1). The modelled patient geometry is therefore a 3D matrix of size 256 × 256 × 40 (565.5 × 565.5 × 400 mm^3).

When the virtual gamma camera following auto-contouring motion approaches the patient model as close as possible, the gamma camera head may collide with the patient geometry in the GATE environment. To prevent this “virtual” collision (as overlapping volumes are not allowed in GATE geometry description), we developed a specific approach that allows non-circular orbit modelling. This work is currently under review [18] and will only be briefly presented here.

A tessellated description of the patient geometry was introduced. This allows the extraction of the volumes of interest (VOI) in fine triangular meshes thereby eliminating the air surrounding the patient responsible for potential virtual collisions. The labelled map was used to further extract mesh surfaces individually for each VOI with a dedicated python script. All the individual meshes were then refined and simplified in the open source 3D image software Blender [19], and stereolithography (.stl) files were exported for each volume. These mesh surfaces were imported in GATE, and materials were added to each volume in conjunction with the patient CT information.

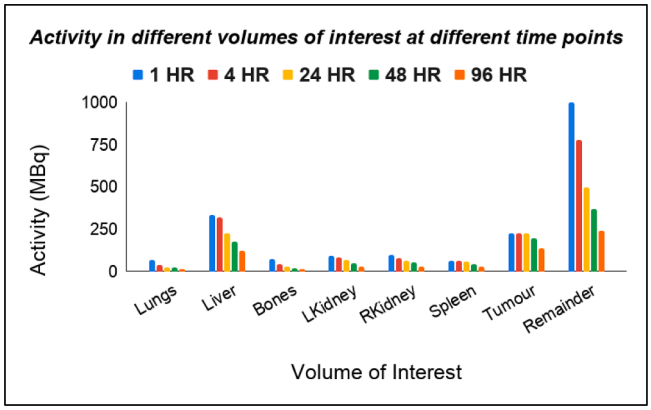


Fig. 1. Activities (in MBq) at each time point (in hours) for the segmented volumes of interest.

Tessellated or mesh-based patient models were therefore generated for each time point from their respective voxelised labelled CT image. This allowed the consideration of changes in patient posture and organ volumes and positioning from one time point to the other, thereby increasing the realism of the modelled dataset.

2.4. Source modelling

2.4.1. Definition of activity map

Activity maps obtained from reconstructed experimental SPECT images along with the calibration factor in Slicer3D toolkit were used for simulations. The mean volumes along with the standard deviation among different time points are stated in Table 2. The use of experimental images allowed the retention of the heterogeneity in activity distribution in the patient at different time points. These heterogeneous activity maps were then post-processed to match the alignment and orientation of the patient model in the GATE environment.

The activity in each volume of interest derived from the registration and segmentation of the experimental SPECT/CT images acquired at each time point are plotted in Fig. 1. By summing the activities in individual VOIs at different time points, the total activity in the FOV was computed. Total activities derived for each time point at 1 h, 4 h, 24 h,

Table 3
Energy of the gamma photons with their respective yields used in simulations.

Energy (in keV)	Yield (in %)
71.6	0.15
112.9	6.40
136.7	0.05
208.4	11.00
249.7	0.21
321.3	0.22

Table 4
Activities at different time points with the corresponding primaries used in the simulations.

Time (in h)	Activity (MBq)	Primaries (Bq. s)
1	1960	318×10^9
4	1687	274×10^9
24	1193	194×10^9
48	930	151×10^9
96	613	99.60×10^9

48 h and 96 h were 1960, 1687, 1193, 930 and 613 MBq respectively. This was then used to calculate the total number of primaries (or particles) to be simulated at each time point.

2.4.2. Source definition, physics list used for the simulations and output

^{177}Lu decays to ^{177}Hf by beta emissions which further emits a range of gamma radiation with two main energy peaks observed at 112.9 keV (6.4%) and 208 keV (11%) [20]. Since only gamma photons contribute to image generation, 0.18033 emissions per decay was considered for the simulations. Table 3 shows the yield corresponding to each energy of gamma photons [21].

For the simulation of phantom images, this meant generating 17.50 $\times$ 10^9 primaries (corresponding to the activity of 107.83 MBq in the total phantom).

For patient images, the activity present in the field of view at each time point along with the corresponding primaries are summarised in Table 4.

The electromagnetic Geant4 physics list used in GATE was emstandard_opt3 [9,22].

The simulation output was stored in ROOT files containing information on the particle id, position, direction and interaction type, that further permits SPECT projections to be generated for different spectrometric energy windows in the simulated energy range.

2.5. Comparison metrics (projections)

To validate the simulated SPECT projections against experimental SPECT projections, several criteria were considered:

- *Flattened profiles*:

For the comparison of the slices of 2D SPECT projections, flattened 1D profiles on the x-axis were created (for each projection) using a python script by summing all the counts along the y-axis.

- *Gamma Index:*

Gamma Index was used as a comparison metric to compare images as it accounts for both difference in counts (Dose Difference or DD criteria) and spatial difference (Distance to Agreement or DTA) [23,24].

Gamma index pass rate (GIPR), a pass/fail criterion specifies a percentage of gamma less than 1 (indicating the points lying within the given DD/DTA acceptance criteria) [25].

2.6. Reconstruction

Every clinical workstation uses DICOM (*Digital Imaging and Communications in Medicine*) files consisting of a raw image i.e. a 3D matrix representing the image and a header file with a standardised series of tags containing information relating to the patient demographics, acquisition parameters, image dimensions, matrix size, colour space, and a host of additional information. The raw image or the pixel intensity data (single or multiple image frames) is attributed to a tag called 'Pixel Data' (7FE0, 0010) in the DICOM file [26,27].

Simulated SPECT projections are raw images that are generated in interfile/projection format (.raw or .hdr/.sin extension). These simulated projections were inserted in the 'Pixel Data' tag of the patient DICOM file and the header information regarding patient and acquisition parameters were kept intact. This was done to test the incorporation of simulated SPECT projections into a vendor-specific and vendor-neutral clinical workstation.

3. Results and discussions

3.1. Calibration images

Experimental and simulated SPECT projections were reconstructed using a Hermes workstation (Hermes Medical Solutions, Sweden) with the same parameters. These OSEM reconstruction parameters include 5 iterations and 16 subsets along with a Gaussian post filter at 0.8 cm and corrected for attenuation (using CT), scatter (using in-built Monte Carlo scatter correction) and collimator-detector response (default). Calibration factors were derived using the expression:

$$Calibration\ factor\ \left(CF\right) = \frac{Counts_{VOI}}{Activity\ \left(A_0\right)\ \times\ time_{acq}}$$

The experimental calibration factor was 5.33 $\pm$ 0.27 cps/MBq while the calibration factor obtained from simulated images was 6.40 cps/MBq. The ratio of 20.1% between simulated and experimental calibration factor is not surprising as the virtual gamma camera sensitivity is

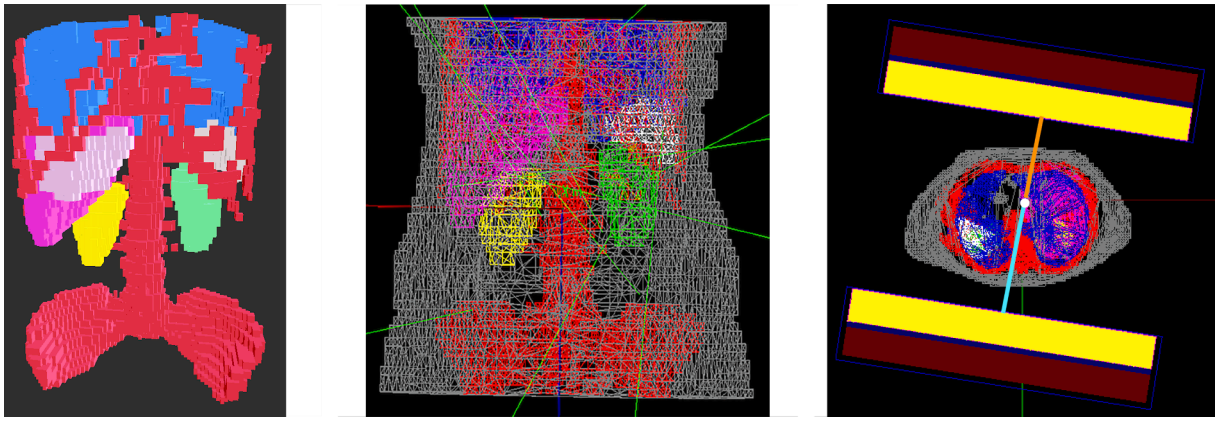


Fig. 2. Visualisation of the patient mesh model with different volumes of interest - bones (in red), lungs (in blue), liver (in pink), spleen (in white), left and right kidney (in green and yellow respectively) a) in Blender and b) in GATE along with the remainder of the body (in grey). The green lines represent the photons emissions in GATE. c) Visualisation of the auto contouring GE Infinia gamma camera motion in GATE. (For interpretation of the references to colour in this figure legend, the reader is referred to the web version of this article.)

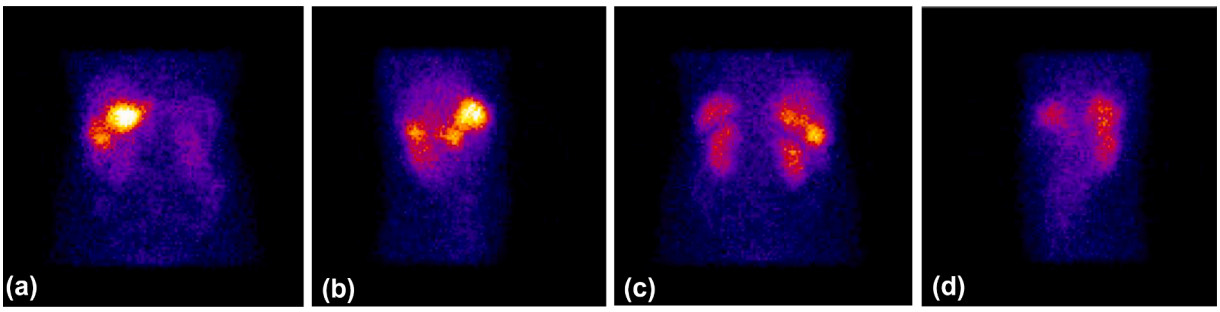


Fig. 3. Simulated SPECT projections as the gamma camera rotates around the patient model - from left to right the angles are 0°, 90°, 180°, 270° respectively. The tumour in the liver having the highest activity can be seen in the projections along with lower activities in kidneys and spleen.

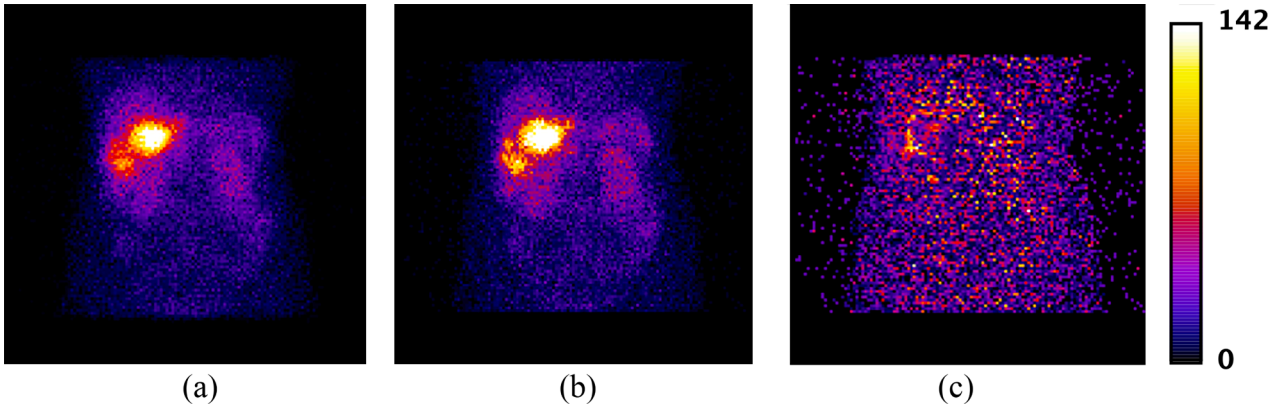


Fig. 4. Simulated (a) and clinical (b) patient SPECT projections 1-hour post injection along with the gamma index map (with gamma index ranging from 0 to 0.1) (c).

usually higher than that of the real gamma camera. This illustrates the importance of deriving a simulation-specific calibration factor to quantify the activity in simulated SPECT images. This calibration factor ratio is further used for adjusting the simulated patient images for comparison with the experimental images and will be referred to as *sensitivity ratio*.

3.2. Clinical images

3.2.1. Simulated patient SPECT projections

The simulated projections of the patient model (Fig. 2a) were generated with realistic activities by implementing the auto-contouring motion of the detector head (Fig. 2b). It can be seen from the figure that the two heads are not equidistant from the centre of the rotation (the unequal distance in orange and blue). SPECT projections at different gamma camera positions are shown in Fig. 3.

3.2.2. Comparison of simulated and experimental patient images

These modelled SPECT projections were compared against the experimental patient projections. As illustrated in Fig. 4, the simulated projections qualitatively look already very similar to the experimental images.

Flattened 1D profiles were made to compare these images at different gamma camera positions (Fig. 5). The simulated projections were normalised with the sensitivity ratio derived from the calibration images. These profiles highlight the accurate positioning and alignment of the patient and gamma camera with respect to the centre of rotation between simulations and experiments.

Comparison of this dataset was performed using a gamma index considering 2% – 1 pixel criteria. Gamma index passing rate was 95.5% with an average gamma of 0.35 (for the images at 1-hour post injection) indicating high similarity between experimental and simulated images. The difference in the total counts between experimental and simulated patient images (considering the sensitivity ratio) at 1-hour post injection was around 2%.

Further, simulated SPECT patient projections were also generated for all the remaining time points i.e., 4 h, 24 h, 48 h and 96 h post injection thus enabling the modelling of activity distribution within the patient over time, the estimation of cumulated activity and absorbed dose calculation. Fig. 6 shows the simulated SPECT projections at these time points.

These simulated projections at 4 h, 24 h, 48 h and 96 h post injection were also compared against the respective clinically acquired patient images using gamma index metric with same criteria as for the projections at 1-hour post injection. Gamma index passing rate ranged from 95% to 98% and the average gamma between 0.28 and 0.35 among different time point thus indicating high similarity between images. The difference in total counts between experiments and simulations (considering the sensitivity ratio) was less than 6% among different time points.

3.3. Computation time

Simulation of SPECT projections with realistic activities in a therapeutic context (1-hour post injection) took 11.5 h to compute using 3560 CPU cores at the regional high-performance computing (HPC) centre CALMIP [28] (instead of 9.59 years with a single CPU core with 2,6GHz, 16 GB), thus making it feasible to generate simulated SPECT images for the virtual multicentric clinical dosimetry trial.

3.4. Reconstruction

3.4.1. Reconstruction with Hermes

Simulated SPECT images integrated into the experimental Infinia patient DICOM headers were successfully accepted by the vendor-neutral Hermes workstation.

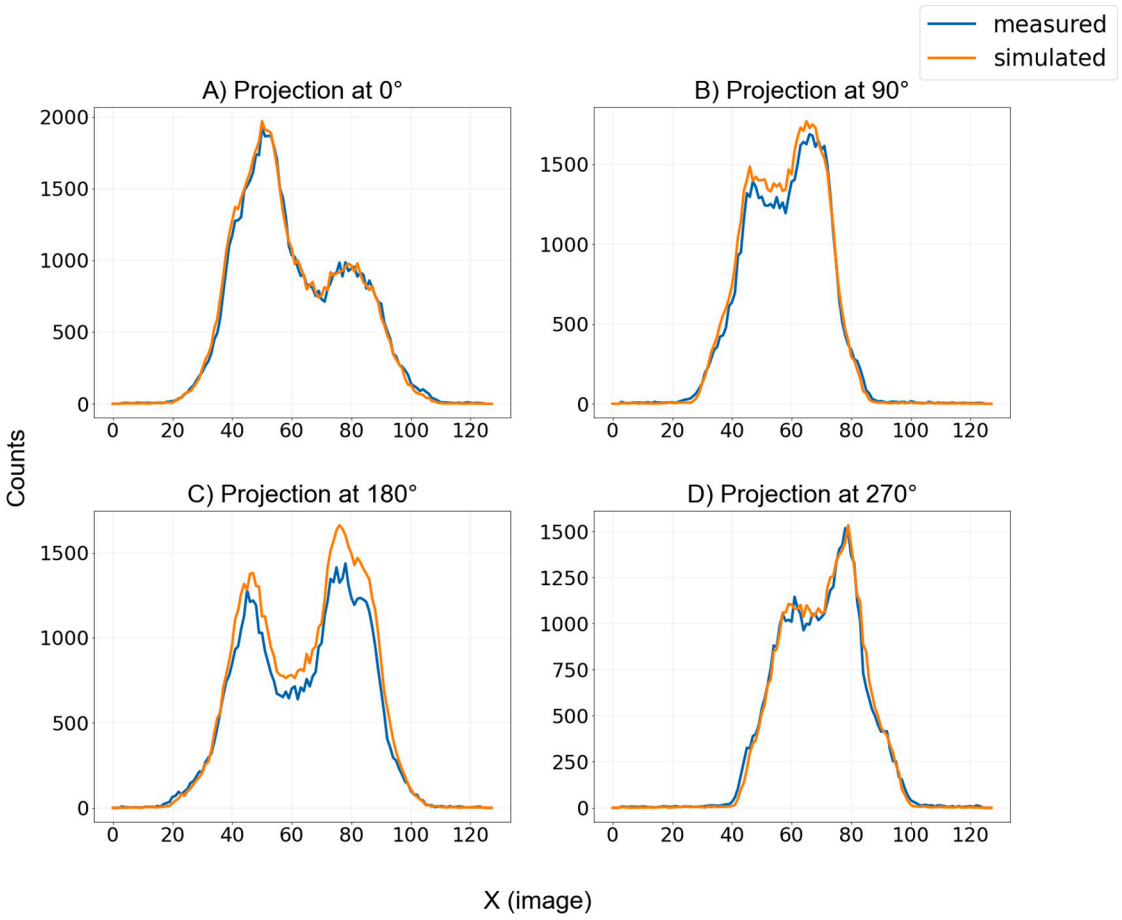


Fig. 5. Flattened profiles on x-axis for comparison of clinical and simulated images at different projection angles - (A) 0°, (B) 90°, (C) 180°, (D) 270°.

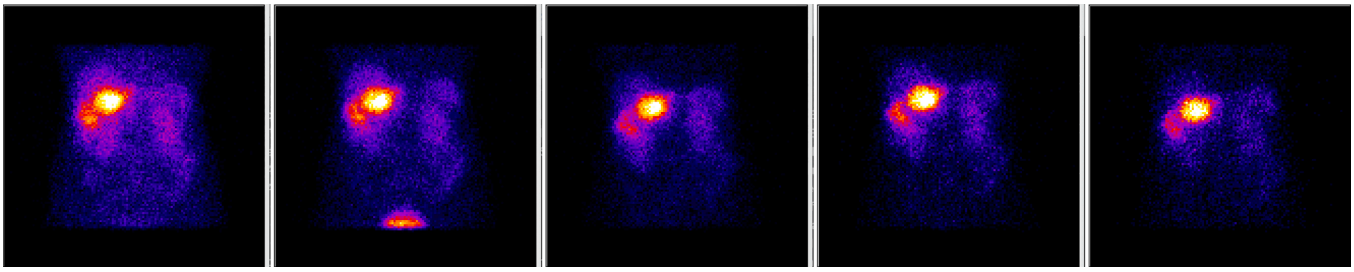


Fig. 6. Simulated patient SPECT projections at different time points post injection (p.i.).

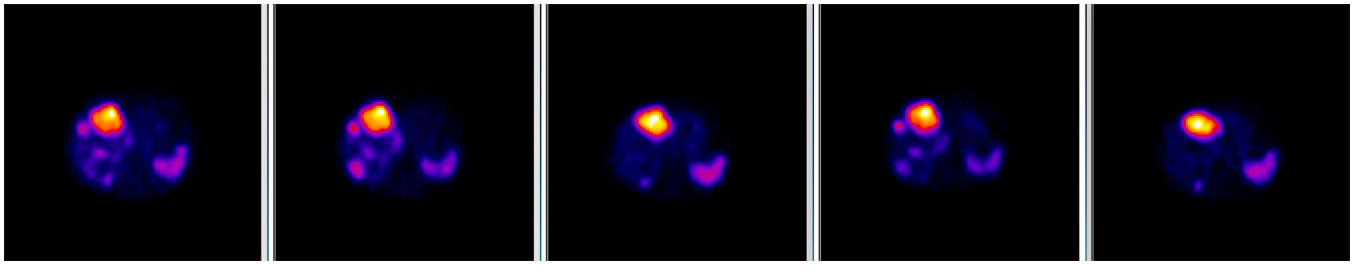


Fig. 7. Reconstructed simulated SPECT images on Hermes at different time points post injection (p.i.)

These simulated SPECT images (.dcm) along with the patient CT were used as an input into the Hybrid dosimetry module™ (HDM) from HERMES Medical Solutions (Version 1.0) available in our laboratory. Reconstruction of the dataset was performed using the HybridRecon-Oncology version_1.3_Dicom (HROD) with the main ^{177}Lu spectrometric energy window of 208 keV. All images were reconstructed with an OSEM reconstruction algorithm with 5 iterations and 16 subsets along with a Gaussian post filter at 0.8 cm. Corrections including CT-

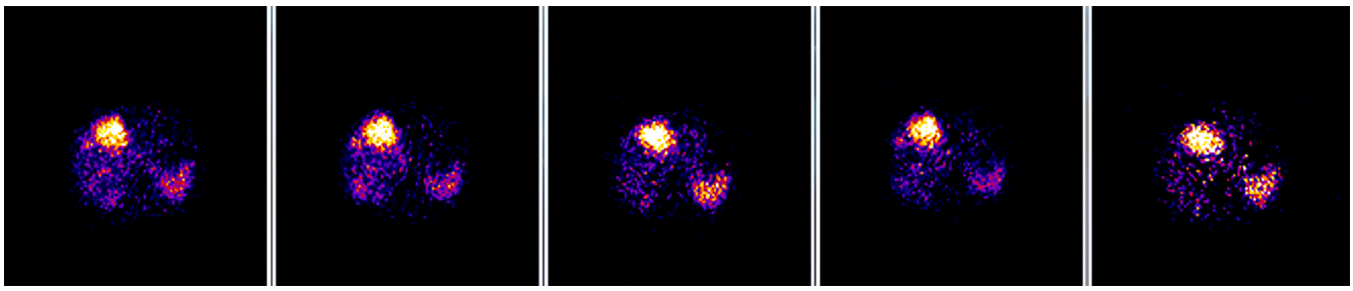


Fig. 8. Reconstructed simulated SPECT images on Xeleris at different time points post injection (p.i.)

based attenuation correction, manufacturer-based Monte Carlo scatter correction and collimator-detector response corrections were applied. Our workstation did not have the SPECT standard uptake value (SUV) option at the time of this work [29]. All SPECT reconstructed images have a matrix size of 128 × 128 with 120 slices and voxel size of 4.42 × 4.42 × 4.42 mm^3.

Fig. 7 shows the reconstructed SPECT images corresponding to different times post injection.

3.4.2. *Reconstruction with Xeleris™*

Simulated SPECT projections integrated into the experimental Infinia patient DICOM headers for all time points post injection were successfully accepted by the vendor-specific Xeleris workstation.

Reconstruction of the simulated SPECT images was performed with Xeleris™ software from GE Healthcare (v3.0513) at ICO, Nantes, France. Images were reconstructed using the OSEM algorithm (5 iterations, 16 subsets). Attenuation correction was performed with appropriate attenuation maps derived from the CT dataset. To account for the TEW scatter correction, projections corresponding to the lower scatter of ^{177}Lu i.e. 178 keV ± 5% and an upper scatter of ^{177}Lu i.e. 241 keV ± 5% were generated from the root file as explained in Section 2.6 and subtractive method was applied [30]. All SPECT reconstructed images have a matrix size of 128 × 128 with 120 slices and voxel size of 4.42 × 4.42 × 4.42 mm^3. Fig. 8 shows the reconstructed SPECT images in Xeleris corresponding to different times post injection.

The simulated SPECT projections reconstructed with Xeleris were noisier compared with the reconstructed images from Hermes. This ratio can be explained by the fact that the reconstruction parameters were not identical on the two workstations. Additionally, the implementation of scatter correction in Hermes is Monte Carlo based with the main energy window, whereas in Xeleris a TEW subtractive method with three energy windows is performed which contributes to the noise generation. Moreover, the resolution recovery correction could not be accounted for in Xeleris, which also contributes to observed differences in the reconstructed images.

Comparison of the reconstruction algorithms implemented in each workstation is beyond the scope of this work. However, it should be noted that for a given workstation, it is advisable that the experimental calibration phantom images along with the patient SPECT projections be reconstructed in the same way. Then, the calibration factor should be derived for each workstation and used with patient images for the quantification of activities in different volumes of interest. Activity quantification should at the end yield similar results between different workstations. This will be further investigated within the DosiTest project.

Yet, it must be noted that it was possible to reconstruct the GATE simulated SPECT projections in two commercial workstations (Hermes and Xeleris) provided that they are correctly integrated in the DICOM headers accepted by these workstations.

4. Conclusions

A realistic simulation of ^{177}Lu clinical datasets (patient SPECT images) was generated with realistic activities in a therapeutic context. These modelled datasets will be further circulated to different clinical departments to perform dosimetry.

The dosimetric analysis of our simulated data will be performed in different clinical departments as part of the IAEA CRP project E23005. This will prove the feasibility of the DosiTest project.

Further work is needed to determine if and how simulated images can be provided for the whole range of gamma camera manufacturers (GE, Siemens, Philips or Mediso). At this stage, it is not clear if the problem can be solved by transcoding the simulated data in another proprietary format, or if a specific modelling of each gamma camera is needed.

Yet, the objective is to generate a set of modelled images (planar, SPECT/CT), at different time points, for different gamma cameras, for the *same* virtual patient and pharmacokinetics, thereby allowing the comparison between different dosimetric approaches.

Declaration of Competing Interest

The authors declare that they have no known competing financial interests or personal relationships that could have appeared to influence the work reported in this paper.

Acknowledgement

The patient images used were obtained as a part of *IAEA Coordinated Research Project (CRP) on "Dosimetry in Radiopharmaceutical therapy for personalized patient treatment" (E2.30.05)*.

The author expresses sincere gratitude to *Mr. Eli Stern* from GE Healthcare, Israel for generating attenuation maps and *Dr Gian Luca Poli* from IAEA, Austria for their active participation and constant support.

This work was granted access to the HPC resources of CALMIP supercomputing centre under the allocation 2016-P19001.

Funding

OpenDose3D module in Slicer3D toolkit has been developed as a part of the Medirad project, which received funding from the Euratom research and training programme 2014-2018 under grant agreement No. 755523. This work has been partially funded by the ENEN + project that has received funding from the Euratom research and training Work programme 2016-2017-1 #75576.

Appendix A. Supplementary data

Supplementary data to this article can be found online at https://doi.org/10.1016/j.ejmp.2021.04.002.

References:

[1] International Atomic Energy Agency (IAEA), Dosimetry in Molecular Radiotherapy for Personalized Patient Treatments; https://www.iaea.org/projects/crp/e23005; 2020 [accessed 01 November 2020].

[2] Gear JI, Cox MG, Gustafsson J, Gleisner KS, Murray I, Glatting G, et al. EANM practical guidance on uncertainty analysis for molecular radiotherapy absorbed dose calculations. Eur J Nucl Med Mol Imaging 2018;45(13):2456–74. https://doi.org/10.1007/s00259-018-4136-7.

[3] DosiTest project, www.dositest.com; 2020 [accessed 01 November 2020].

[4] Garcia M-P, Villoing D, McKay E, Ferrer L, Cremonesi M, Botta F, et al. TestDose: A nuclear medicine software based on Monte Carlo modeling for generating gamma camera acquisitions and dosimetry. Med Phys 2015;42(12):6885–94. https://doi.org/10.1118/1.4934828.

[5] Rogers DWO. Fifty years of Monte Carlo simulations for medical physics. Phys Med Biol 2006;51(13):R287–301. https://doi.org/10.1088/0031-9155/51/13/R17.

[6] Fahey FH, Grogg K, El Fakhri G. Use of Monte Carlo Techniques in Nuclear Medicine. J American College of Radiology. 2018;15(3 Pt A):446-448. 10.1016/j.jacr.2017.09.045.

[7] Buvat I, Castiglioni I. Monte Carlo simulations in SPET and PET. Q J Nucl Med 2002;46(1):48–61.

[8] Ljungberg M, Strand SE, King MA. Monte Carlo calculations in nuclear medicine. 2nd ed. CRC Press; 2012.

[9] Jan S, Santin G, Strul D, Staelens S, Assié K, Autret D, et al. GATE: a simulation toolkit for PET and SPECT. Phys Med Biol 2004;49(19):4543–61. https://doi.org/10.1088/0031-9155/49/19/007.

[10] Sarrut D, Bardiès M, Boussion N, Freud N, Jan S, Létang J-M, et al. A review of the use and potential of the GATE Monte Carlo simulation code for radiation therapy and dosimetry applications. Med Phys 2014;41(6Part1):064301. https://doi.org/10.1118/1.487161710.1118/1.4871617.

[11] Costa GCA, Bonifácio DAB, Sarrut D, Cajgfinger T, Bardiès M. Optimization of GATE simulations for whole-body planar scintigraphic acquisitions using the XCAT male phantom with ^{177}Lu-DOTATATE biokinetics in a Siemens Symbia T2. Phys Med 2017;42:292–7. https://doi.org/10.1016/j.ejmp.2017.07.009.

[12] Rault E, Staelens S, Van Holen R, De Beenhouwer J, Vandenberghe S. Accurate Monte Carlo modelling of the back compartments of SPECT cameras. Phys Med Biol. 2011 Jan 7;56(1):87–104. https://doi.org/10.1088/0031-9155/56/1/006. Epub 2010 Nov 30 PMID: 21119230.

[13] Zhao W, Esquinas PL, Hou X, Uribe CF, Gonzalez M, Beauregard J-M, et al. Determination of gamma camera calibration factors for quantitation of therapeutic radioisotopes. EJNMMI Phy 2018;5(1). https://doi.org/10.1186/s40658-018-0208-9.

[14] Vergara-Gil A, Amato E, Auditore L, Brenet M, Chauvin M, Clayton N et al. OpenDose3D: A free, collaborative 3D Slicer module for patient-specific dosimetry. EANM 2020 (Online).

[15] Pinter C, Lasso A, Wang An, Jaffray D, Fichtinger G. SlicerRT: Radiation therapy research toolkit for 3D Slicer. Med Phys 2012;39(10):6332–8. https://doi.org/10.1118/1.4754659.

[16] Fedorov A, Beichel R, Kalpathy-Cramer J, Finet J, Fillion-Robin J-C, Pujol S, et al. 3D Slicer as an image computing platform for the Quantitative Imaging Network. Magn Reson Imaging 2012;30(9):1323–41. https://doi.org/10.1016/j.mri.2012.05.001.

[17] H. W. Meijering E, J. Niessen W, P. W. Pluim J, A. Viergever M. Quantitative Comparison of Sinc-Approximating Kernels for Medical Image Interpolation. MICCAI 1999, pp. 210-217.

[18] Kayal G, Chauvin M, Mora-Ramirez E, Clayton N, Vergara-Gil A, Tran-Gia J et.al. Modelling SPECT auto-contouring acquisition for 177Lu & 131I Molecular Radiotherapy using new developments in Geant4/GATE. (Submitted).

[19] Bücking Thore M, Hill Emma R, Robertson James L, Maneas Efthymios, Plumb Andrew A, Nikitichev Daniil I, et al. From medical imaging data to 3D printed anatomical models. PLoS One 2017;12(5):e0178540. https://doi.org/10.1371/journal.pone.0178540.

[20] National Nuclear Data Center, MIRD format, https://www.nndc.bnl.gov/nudat2/mird/; 2020 [accessed 03 November 2020].

[21] Eckerman KF, Endo A. MIRD: Radionuclide data and decay schemes. 2nd ed. Reston, VA: Society of Nuclear Medicine; 2008.

[22] Geant4 User Guide, Electromagnetic Physics Constructor; https://geant4-userdoc.web.cern.ch/geant4-userdoc/UsersGuides/PhysicsListGuide/html/electromagnetic/Opt3.html; 2020 [accessed 03 November 2020].

[23] Low Daniel A. Gamma dose distribution evaluation tool. J Phys Conf Ser 2010;250:012071. https://doi.org/10.1088/1742-6596/250/1/012071.

[24] Wendling Markus, Zijp Lambert J, McDermott Leah N, Smit Ewoud J, Sonke Jan-Jakob, Mijnheer Ben J, et al. A fast algorithm for gamma evaluation in 3D. Med Phys 2007;34(5):1647–54. https://doi.org/10.1118/1.2721657.

[25] Hussein Mohammad, Rowshanfarzad Pejman, Ebert Martin A, Nisbet Andrew, Clark Catharine H. A comparison of the gamma index analysis in various commercial IMRT/VMAT QA systems. Radiother Oncol 2013;109(3):370–6. https://doi.org/10.1016/j.radonc.2013.08.048.

[26] Varma RD. Managing DICOM images: Tips and tricks for the radiologist. Indian J Radiol Imaging 2012;22(1):4–13. https://doi.org/10.4103/0971-3026.95396.

[27] Bidgood WD, C. Horii S, W. Prior F, Van Syckle DE. Understanding and using DICOM, the data interchange standard for biomedical imaging. J Am Med Informatics Assoc. 1997;4(3): 199-212. 10.1136/jamia.1997.0040199.

[28] CALMIP, https://www.calmip.univ-toulouse.fr/ ; 2004-2020 [accessed 01 November 2020].

[29] Mora-Ramirez Erick, Santoro Lore, Cassol Emmanuelle, Ocampo-Ramos Juan C, Clayton Naomi, Kayal Gunjan, et al. Comparison of commercial dosimetric software platforms in patients treated with ^{177}Lu-DOTATATE for peptide receptor radionuclide therapy. Med. Phys. 2020;47(9):4602–15.

[30] Ljungberg M, Celler A, Konijnenberg M, Eckerman KF, Dewaraja YK, Sjögreen-Gleisner K et al. MIRD Pamphlet No. 26: Joint EANM/MIRD Guidelines for Quantitative 177Lu SPECT Applied for Dosimetry of Radiopharmaceutical Therapy. J Nucl Med. 2016;57(1): 151-62 10.2967/jnumed.115.159012.